Research Square

Preprints are preliminary reports that have not undergone peer review.
They should not be considered conclusive, used to inform clinical practice,
or referenced by the media as validated information.

TMEM45A Mediates Gastric Cancer Progression Through the P4HA1/Succinate/TGF-β Pathway

Fei Ge
Affiliated Hospital of Nantong University
Rui Ji
Affiliated Hospital of Nantong University
Rongrong Jing
Affiliated Hospital of Nantong University
Yan Wang
Affiliated Hospital of Nantong University
Ming Cui
Affiliated Hospital of Nantong University
Jingchun Wang
wangjingchun0926@163.com
Affiliated Hospital of Nantong University

Article

Keywords: Gastric cancer, TMEM45A, P4HA1, Succinate, TGF-β

Posted Date: July 15th, 2026

DOI: https://doi.org/10.21203/rs.3.rs-10246017/v1

License: This work is licensed under a Creative Commons Attribution 4.0 International License.
Read Full License

Additional Declarations: No competing interests reported.

Abstract

Background

Gastric cancer (GC) generally presents with poor prognosis owing to late diagnosis. Transmembrane protein 45A (TMEM45A) is involved in the progression of various tumors, yet its function and molecular mechanism in GC remain unclear.

Methods

We screened candidate genes via public bioinformatics databases, validated TMEM45A expression by immunohistochemistry in 75 paired GC tissues, and conducted in vitro functional assays and rescue experiments to explore the underlying mechanism.

Results

TMEM45A was significantly upregulated in GC tissues. Its high expression was associated with postoperative residual tumor and poor treatment response, and acted as an independent poor prognostic factor for GC. A nomogram incorporating TMEM45A exhibited favorable accuracy in predicting GC patients' long-term survival. Mechanistically, TMEM45A promoted GC cell proliferation, migration and invasion by physically interacting with and positively regulating P4HA1, elevating succinate levels and activating the TGF-β/Smad pathway; reintroduction of P4HA1 effectively reversed the tumor-inhibitory effects caused by TMEM45A knockdown.

Conclusion

TMEM45A is a novel independent prognostic biomarker for GC. It drives GC progression via the P4HA1-mediated succinate/TGF-β/Smad pathway, and may serve as a promising therapeutic target.

Highlights

Key findings

• TMEM45A is markedly upregulated in gastric cancer (GC) and acts as an independent adverse prognostic factor.

• TMEM45A facilitates GC cell proliferation, migration and invasion via binding to P4HA1, increasing succinate levels and activating the TGF-β/Smad pathway.

What is known and what is new?

• TMEM45A participates in progression and chemoresistance of diverse cancers; P4HA1 modulates succinate metabolism and tumor metastasis.

• This work first validates TMEM45A as a novel prognostic biomarker for GC, and reveals the previously unreported TMEM45A/P4HA1/succinate/TGF-β regulatory axis driving GC progression.

What is the implication, and what should change now?

• TMEM45A is applicable for GC prognostic stratification and represents a promising therapeutic target. In vivo verification and translational research targeting this axis are warranted to optimize GC clinical management.

Introduction

GC is a malignant tumor originating from the gastric mucosal epithelium, with persistently high incidence and mortality rates, thus posing a continuous threat to human health and life [1]. Although advances have been made in early diagnosis, the disease is often asymptomatic in its initial stages, and most patients are diagnosed at an advanced stage, resulting in poor prognosis [2–4]. Existing studies have indicated that the development of GC is typically associated with genetic predisposition, *Helicobacter pylori* infection, and precancerous lesions [2,5]. However, the pathogenesis of GC is multifactorial and complex. Therefore, elucidating the mechanisms underlying GC initiation and progression is essential not only for improving diagnostic accuracy but also for identifying novel therapeutic strategies [6–8]. With the development of bioinformatics and molecular technologies, the identification and discovery of novel key genes involved in GC initiation and progression have become crucial.

TMEM45A (also known as DNAPTP4, FLJ10134, or DERP7) is a multi-pass membrane protein belonging to the large family of transmembrane proteins (TMEM), located on chromosome 3q12.2. It encodes a transmembrane protein consisting of 275 amino acids with five or seven transmembrane domains [9]. Initially, TMEM45A was found to be highly expressed in epidermal keratinocytes, where it is involved in epidermal keratinization [10]. Subsequent studies have reported a strong association between TMEM45A and the progression of various cancers, as well as its role in chemotherapy resistance. For instance, downregulation of TMEM45A has been shown to inhibit the proliferation, migration, and invasion of glioma cells [11]; TMEM45A was critical for hypoxia-induced chemotherapy resistance in breast cancer and liver cancer cells [12]; in HPV-positive cervical cancer cells, inhibition of TMEM45A suppressed cell proliferation, invasion, migration, Epithelial -Mesenchymal Transition (EMT), regulates cell cycle distribution, promotes apoptosis, and reverses cisplatin resistance, providing a potential therapeutic strategy for HPV-positive cervical cancer [13]. Furthermore, high expression of TMEM45A in clear cell renal cell carcinoma promotes EMT and inflammation, acting as a tumor promoter in clear cell renal cell carcinoma [14]. These findings suggest that TMEM45A can regulate the progression of certain tumors, but its regulatory mechanisms in GC remain unclear. Therefore, further investigation is required to clarify the exact function and molecular mechanisms of TMEM45A in GC.

Given the complexity of TMEM45A's role in diseases, we first identified TMEM45A as a key molecule in GC through bioinformatics screening. Subsequently, we validated the relationship between TMEM45A expression and clinicopathological parameters, as well as its value in prognostic prediction, using both bioinformatics and clinical samples. Next, cell experiments were performed to confirm the effect of TMEM45A on the proliferation and metastasis of GC cells. Finally, we identified that TMEM45A regulates GC progression through the P4HA1/succinate/TGF-β pathway (Scheme 1).

Methods and materials

Tissue specimens

Tumor tissues and adjacent normal tissues from 75 GC patients included in this study were collected at the Affiliated Hospital of Nantong University between January 2013 and December 2014. None of the patients had received chemotherapy or radiotherapy prior to tissue collection. All samples were immediately stored at -80°C. The study was approved by the Ethics Committee of the Affiliated Hospital of Nantong University (2024-K078-01).

Immunohistochemistry assay

GC tissues and corresponding normal tissues were fixed in 4% paraformaldehyde, followed by a series of processes including dehydration, clearing, infiltration, and embedding in paraffin. The paraffin-embedded tissue blocks were sectioned and mounted on glass slides. The slides were baked in an oven for 40 minutes, followed by two washes in xylene. The sections were then immersed in graded ethanol solutions (100%, 90%, 80%, 70%) at room temperature for 5 minutes each. Endogenous peroxidase activity was inhibited by incubating the slides with a peroxidase inhibitor at room temperature in the dark for 10 minutes. After multiple washes with PBST buffer, the diluted primary antibodies (TMEM45A, 1:100, ABmart) were added, and the slides were incubated overnight at 4°C. The following day, the slides were washed three times with PBST buffer and incubated with the secondary antibody at room temperature for 60 minutes. After washing with PBST buffer, DAB was used for color development. The staining reaction was stopped when a brownish-yellow precipitate appeared. All tissue sections were counterstained with hematoxylin. The processed slides were observed and photographed under a microscope. At least five high-power fields were randomly selected for observation and photography. The percentage of the positively stained area relative to the total tumor area was calculated (ranging from 0 to 100). The staining score ranged from 0 (no staining), 1 (light yellow), 2 (brownish tone), to 3 (brownish). The final TMEM45A staining intensity was combined with the percentage of positive cells to obtain a composite score, ranging from 0 to 300.

Cell culture

The human gastric cancer cell lines (HGC-27, AGS) and gastric epithelial cell line (GES-1) were purchased from the Shanghai Cell Bank, Chinese Academy of Sciences. The gastric cancer cell lines (MKN-45) were purchased from Shanghai Zhongqiao Xinzhou Biotechnology Co., Ltd. These cells were cultured in RPMI-1640 medium (Gibco, USA) supplemented with 10% fetal bovine serum (Gibco, USA) and 1% penicillin-streptomycin (Xinsaimei, Suzhou, China). The cell cultures were maintained in a 37°C incubator with 5% CO_2.

Cell transfection

The TMEM45A knockdown and overexpression plasmids, as well as the P4HA1 overexpression plasmid, were designed and synthesized by Gima Biotech Co., Ltd. (Gima, Suzhou, China). The TMEM45A interference sequence used in this experiment was (5'-3'): GGAGCTGGTTCTTTCAGATTG. Cells were seeded at a density of $5{\cdot}10^5$ cells per well in 6-well plates containing serum-supplemented medium. According to the product instructions, plasmid transfection was performed using Lipofectamine™ 3000 (Invitrogen, USA). The cells were incubated in a 37°C, 5% CO_2 incubator for 48 hours before subsequent functional assays.

Total RNA extraction and RT-qPCR experiments

TRIzol reagent (Invitrogen, California, USA) was added to GC tissues and cells for lysis, and total RNA was extracted. The total RNA extracted from gastric cancer tissues and cells was reverse transcribed into cDNA using a reverse transcription kit (Shark Biotechnology, China). PCR amplification was performed using a Roche 480 system (Roche, Germany). Primer sequences were synthesized by Shenggong Biotechnology Co., Ltd. The primers used were as follows: TMEM45A (forward) 5'-GGAGCTATTGCGGTCAAGTC-3'; TMEM45A (reverse) 5'-GGGGATACAGGACAAATCCA-3'; 18S rRNA (forward) 5'-GTAACCCGRRGAACCCCATT-3'; 18S rRNA (reverse) 5'-CCATCCAATCGGTAGTAG-3'. The 20 μL amplification system consisted of 10 μL 2·universal SYBR green fast qPCR mix (ABclonal, Wuhan, China), 5 ng cDNA, 10 μM primers, and an appropriate volume of ddH_2O. The amplification program was as follows: 95°C for 5 minutes; 95°C for 15 seconds; 60°C for 30 seconds; 72°C for 15 seconds. This cycle was repeated for 45 cycles. The relative expression of TMEM45A mRNA was calculated using the $2^{-\Delta\Delta CT}$ method.

Cell Counting Kit-8 (CCK8)

GC cells were seeded in a 96-well plate at a density of 3,000 cells per well and cultured in a 37°C, 5% CO_2 incubator. At 24, 48, 72, 96, and 120 hours, 10 μL of CCK-8 reagent (Shark Biotechnology, China) was added to each well, and the cells were incubated for 2 hours. The absorbance at 450 nm (OD450) was measured using a microplate reader.

Colony formation

GC cells were seeded in a 6-well plate at a density of 1000 cells per well and cultured in a 37°C, 5% CO_2 incubator for 14 days. The cells were washed with PBS and fixed with 4% paraformaldehyde for 30 minutes. After washing three times with PBS, the cells were stained with crystal violet dye solution for 15 minutes. Following PBS washing, the cells were air-dried, and the number of colony-forming units was counted.

EdU proliferation

GC cells were seeded in a 24-well plate at a density of $3 \cdot 10^4$ cells per well and cultured overnight in a 37°C, 5% CO_2 incubator. According to the manufacturer's instructions (Beyotime, China), 1· EDU working solution was prepared and added to the 24-well plate. The cells were incubated at 37°C for 2 hours. The cells were then fixed with 4% paraformaldehyde for 20 minutes. After incubation with 0.3% Triton X-100 at room temperature for 15 minutes, the EDU working solution was added and incubated in the dark at room temperature for 30 minutes. Finally, Hoechst solution was used for staining. The number of positive cells was counted using an inverted fluorescence microscope.

Transwell migration and invasion

In a 24-well plate, 100 μL of cell suspension ($7 \cdot 10^4$ cells) was added to the upper chamber of a Transwell insert (8 μm pore size, Corning, USA) coated with or without Matrigel, and 500 μL of medium containing 20% FBS was added to the lower chamber. The plate was incubated in a 37°C, 5% CO_2 incubator for 48 hours. After incubation, the chambers were washed with PBS, fixed with 4% paraformaldehyde for 20 minutes, and stained with crystal violet dye solution for 10 minutes. Finally, images were captured using an inverted microscope to record the number of cells in the lower chamber.

Wound healing assay

GC cells were seeded in a 6-well plate at a density of $5 \cdot 10^5$ cells per well and cultured overnight in a 37°C, 5% CO_2 incubator. A sterile pipette tip was used to create a scratch on the cell monolayer. The cells were then cultured in serum-free medium and images were captured at 0, 12, and 24 hours using an inverted microscope. The cell migration ability was assessed by measuring the change in the area of the wound.

Immunofluorescence

For immunofluorescence staining, cells were first fixed with 4% paraformaldehyde for 10 minutes, then washed three times with phosphate-buffered saline (PBS). Cells were subsequently fixed with 0.3% Triton X-100-containing fixative for 15 minutes, followed by three PBS washes. After fixation, cells were blocked with 5% bovine serum albumin (BSA) blocking solution at room temperature for 1 hour; blocking solution was removed thereafter. Primary antibodies (TMEM45A, 1:400; P4HA1, 1:200) were added, and

cells incubated overnight at 4°C. The next day, primary antibodies were aspirated, and cells washed three times with PBS. Secondary antibodies (goat anti-rabbit IgG-Alexa Fluor 488, 1:1000, goat anti-mous IgG-Alexa Fluor 580,1:1000) were added, with incubation at RT for 1 hour in the dark to avoid photobleaching. Unbound secondary antibodies were aspirated, followed by three PBS washes. Finally, cell nuclei were stained with DAPI at RT for 5 minutes in the dark, then washed three times with PBS. Stained cells were observed via inverted fluorescence microscope, and images captured for documentation.

Western blot

Proteins were extracted from cells using a protease and phosphatase inhibitor (Sole, Beijing, China) and RIPA lysis buffer (Thermo, USA). The protein lysates were separated by SDS-PAGE and transferred to a PVDF membrane. The membrane was blocked with a rapid blocking buffer (non-protein) for 10 minutes. The diluted primary antibodies (TMEM45A, 1:1000, Proteintech, China; P4HA1, 1:5000, Proteintech, China;Smad2/3, 1:1000, Epizyme, China; p-Smad2/3, 1:1000, Epizyme, China) were incubated overnight at 4°C. The next day, the secondary antibody of the same species was incubated at room temperature for 2 hours. After washing three times, detection was performed using ECL chemiluminescence.

Succinic Acid detection

GC cells were seeded into 6-well plates at a density of 1×10^6 cells per well and cultured overnight in a humidified incubator with 5% CO_2 at 37°C. The working solution was freshly prepared in strict accordance with the manufacturer's instructions provided with the Succinic Acid Assay Kit (Beyotime, China). Subsequently, the working solution was added to 96-well plates, followed by incubation at 37°C in the dark for 30 minutes. The absorbance at a wavelength of 570 nm was detected using a microplate reader. A standard curve was constructed to quantify the concentration of succinic acid in GC cells.

Gene expression dataset application and data sources for predicting prognosis

STAD datasets were downloaded from the GEO database (https://www.ncbi.nlm.nih.gov/geo/), including GSE79973 (10 normal gastric tissue samples and 10 gastric cancer tissue samples), GSE118916 (15 normal and 15 cancer samples), and GSE103236 (9 normal and 10 cancer samples). Differentially expressed genes (DEGs) were identified based on the criteria of $|\log2FC| > 1$ and $P < 0.05$. Kaplan–Meier Plotter (http://kmplot.com/analysis/) was used to perform survival analysis of DEGs in gastric cancer.The expression levels of TMEM45A and P4HA1 were analyzed using RNA-seq data from The Cancer Genome Atlas (TCGA, https://portal.gdc.cancer.gov/), the Genotype-Tissue Expression (GTEx) database (https://www.gtexportal.org/home/index.html), and the UALCAN portal (http://ualcan.path.uab.edu/analysis.html) under the STAD project. The Human Protein Atlas (HPA) (https://www.proteinatlas.org/) was used to evaluate the protein expression levels of TMEM45A and P4HA1. Protein–protein interaction (PPI) networks were constructed using STRING (https://cn.string-db.org/).

Construction of nomogram plots

A nomogram was constructed to evaluate the predictive ability of various factors (age, TNM stage, T stage, N stage, and M stage) for 1-year, 3-year, and 5-year overall survival (OS). The calibration curve, based on the Hosmer-Lemeshow test, was used to verify the consistency between the actual outcomes and the model predictions.

Statistical analysis

Data were analyzed using t-tests, analysis of variance (ANOVA), and chi-square tests with GraphPad Prism 10.0 and SPSS 20.0 software. Results are presented as mean ± standard deviation (Mean ± SD). Kaplan-Meier survival analysis was performed using the "survival" package in R software, and univariate and multivariate analyses were conducted using the Cox proportional hazards stepwise regression model. Statistical significance was defined as a $P < 0.05$.

Results

Screening and validation of key molecules in GC

As shown in Fig. 1, three GC-related datasets (GSE79973, GSE118916, and GSE103236) were retrieved from the GEO database, and intersection analysis of these datasets based on the screening criteria of |log2 FC| > 1 and P < 0.05 revealed a total of 178 genes with significant expression differences. Subsequently, Cox regression analysis (HR ≠ 1 and $P < 0.05$), proportional hazards assumption test ($P > 0.05$), and Kaplan-Meier survival analysis ($P < 0.05$) were performed using data from TCGA database, leading to the identification of 35 differentially expressed genes associated with prognosis. To determine the key genes with independent predictive value for prognostic assessment, Lasso regression analysis was conducted on the aforementioned 35 genes. After validation by 10-fold cross-validation, five key genes were finally screened out: FKBP10, SERPINE1, FNDC1, IGFBP7, and TMEM45A. Given the limited reports on TMEM45A in GC, we selected this gene as a candidate for subsequent research.

TMEM45A is Highly Upregulated in Gastric Cancer and Correlates with Clinical Characteristics

To investigate the expression of TMEM45A in GC, we analyzed data from the TCGA-STAD, GTEx, and UALCAN databases. The results demonstrated that the mRNA level of TMEM45A in GC tissues was significantly higher than that in normal tissues ($P < 0.001$, Fig. 2A-C). To assess the potential of TMEM45A in distinguishing GC tissues from normal tissues, we performed a receiver operating characteristic (ROC) curve analysis (Fig. 2D). The area under the ROC curve (AUC) for TMEM45A was 0.656 (95% CI: 0.609–0.702). Furthermore, we compared the protein levels of TMEM45A in normal human gastric tissues and GC tissues using the HPA database. The results showed that the protein abundance of TMEM45A in GC tissues was significantly higher than in normal tissues (Fig. 2E). To further validate these findings, we conducted immunohistochemical analysis on 75 pairs of clinically collected GC tissues and adjacent normal tissues. The results indicated that the expression of

TMEM45A was significantly higher in GC tissues compared to adjacent normal tissues ($P < 0.0001$, Fig. 2F). Meanwhile, through analyzing the correlation between TMEM45A expression and the clinical characteristics of GC patients, we found that the expression level of TMEM45A was significantly associated with residual tumor status and initial treatment outcomes of GC ($P < 0.05$) (Table 1). In conclusion, TMEM45A expression is upregulated in GC tissues.

Table 1
TMEM45A expression and clinical features in GC patient samples.

Characteristics	TMEM45A		P value
	Low	High	
n	187	188	
Gender, n (%)			0.695
Male	122 (32.5%)	119 (31.7%)	
Female	65 (17.3%)	69 (18.4%)	
Age, n (%)			0.963
<= 65	82 (22.1%)	82 (22.1%)	
> 65	103 (27.8%)	104 (28%)	
Pathologic T stage, n (%)			0.548
T1-T2	53 (14.4%)	46 (12.5%)	
T3-T4	134 (36.5%)	134 (36.5%)	
Pathologic N stage, n (%)			0.793
N0	56 (19.9%)	55 (19.5%)	
N1-N3	89 (31.6%)	82 (29.1%)	
Pathologic M stage, n (%)			0.142
M0	169 (47.6%)	161 (45.4%)	
M1	9 (2.5%)	16 (4.5%)	
Pathologic stage, n (%)			0.754
Stage I-Stage II	81 (23%)	83 (23.6%)	
Stage III-Stage IV	96 (27.3%)	92 (26.1%)	
Residual tumor, n (%)			**0.019***
R0	162 (49.2%)	136 (41.3%)	
R1	7 (2.1%)	8 (2.4%)	
R2	3 (0.9%)	13 (4%)	
H pylori infection, n (%)			0.276
No	84 (51.5%)	61 (37.4%)	

Characteristics	TMEM45A		P value
	Low	High	
Yes	8 (4.9%)	10 (6.1%)	
Primary therapy outcome, n (%)			**0.038***
PD	27 (8.5%)	38 (12%)	
SD	11 (3.5%)	6 (1.9%)	
PR	0 (0%)	4 (1.3%)	
CR	124 (39.1%)	107 (33.8%)	

TMEM45A Serves as a Prognostic Marker in Gastric Cancer

To explore the impact of TMEM45A expression levels on the survival of GC patients, we performed univariate and multivariate Cox regression analyses on GC patients with complete pathological characteristics from the TCGA database. Univariate Cox regression analysis showed that factors affecting GC survival included stage ($P < 0.001$, HR = 1.607), N stage ($P < 0.001$, HR = 1.342), M stage ($P = 0.004$, HR = 2.303), T stage ($P = 0.01$, HR = 1.319), age ($P = 0.025$, HR = 1.018), and TMEM45A expression levels ($P = 0.036$, HR = 1.23) (Fig. 3A). Multivariate Cox regression analysis further revealed that stage ($P < 0.001$, HR = 1.722), age ($P = 0.003$, HR = 1.026), and TMEM45A expression levels ($P = 0.069$, HR = 1.209) were independent factors affecting the survival of GC patients (Fig. 3B). These results suggest that high expression of TMEM45A may serve as an independent prognostic factor for GC patients.

To more accurately predict the prognosis of GC patients, a nomogram was constructed incorporating age, stage, and TMEM45A expression levels (Fig. 3C). In this model, each risk factor was assigned a corresponding score, and a risk classification system was established based on the total score obtained by patients in the model, with the median score serving as the threshold. To further validate the predictive ability of the nomogram model, we plotted time-dependent ROC curves for overall survival (OS). The model showed prognostic accuracy rates of 0.667, 0.625, and 0.666 for 1-year, 3-year, and 5-year OS, respectively (Fig. 3D). Furthermore, the calibration curves for 1-year, 3-year, and 5-year OS predicted by the nomogram closely aligned with the reference line, indicating that the model has good predictive precision and reliability (Fig. 3E). In summary, the nomogram model we constructed can more accurately predict the prognosis of GC patients.

TMEM45A Promotes Proliferation, Migration, and Invasion in Gastric Cancer

To investigate the effect of TMEM45A on the proliferation, migration, and invasion capabilities of GC cells, we performed in vitro cell experiments. First, we determined the expression level of TMEM45A in five GC cell lines (Fig. 4A). As a result, we selected AGS ($P < 0.0001$) and HGC-27 ($P < 0.05$) cells, which showed moderate TMEM45A expression, for subsequent experiments. Subsequently, TMEM45A knockdown plasmids and TMEM45A overexpression plasmids were transfected into AGS and HGC-27 cells, respectively. RT-qPCR results demonstrated that the expression level of TMEM45A was significantly decreased in GC cells transfected with TMEM45A knockdown plasmids (AGS, $P < 0.0001$; HGC-27, $P < 0.001$; Fig. 4B). In contrast, the expression level of TMEM45A was remarkably increased in GC cells transfected with TMEM45A overexpression plasmids (AGS, $P < 0.01$; HGC-27, $P < 0.0001$; Fig. 4C). Results from colony formation assay, EdU assay, and CCK-8 assay showed that the proliferation ability of GC cells with TMEM45A knockdown was significantly lower than that of control cells, whereas GC cells with TMEM45A overexpression exhibited enhanced proliferation ability (Fig. 4D-I). Additionally, Transwell assay and wound healing assay results revealed that when TMEM45A was knocked down, the migration and invasion capabilities of GC cells were significantly reduced; in contrast, the migration and invasion capabilities of GC cells with TMEM45A overexpression were significantly higher than those of control cells (Fig. 4J-M). These results indicated that TMEM45A promotes the proliferation, migration, and invasion of GC cells.

TMEM45A Binds to P4HA1 to Promote the Proliferative, Migratory, and Invasive Capabilities of GC

To identify potential factors associated with TMEM45A, we constructed a Protein-Protein Interaction (PPI) network using the STRING database. The results revealed 4 distinct genes associated with TMEM45A (Fig. 5A). Based on the combined score, P4HA1 exhibited the strongest binding affinity to TMEM45A (Fig. 5B). Consequently, we employed immunofluorescence staining to evaluate the co-localization of TMEM45A and P4HA1 expression in GC cells. The results demonstrated that TMEM45A and P4HA1 were co-localized in AGS and HGC-27 cells (Fig. 5C). To investigate the expression pattern of P4HA1 in GC, we analyzed data from the TCGA and HPA databases, which showed that the expression level of P4HA1 in GC tissues was significantly higher than that in normal gastric tissues (Fig. 5D-E). Meanwhile, Kaplan-Meier survival analysis indicated that elevated P4HA1 expression was associated with poor prognosis ($P = 0.035$) (Fig. 5F). Correlation analysis between P4HA1 and TMEM45A was performed using the Timer database, and the results showed a positive correlation between the two molecules (Fig. 5G). Furthermore, Western Blot experiments confirmed this finding: we observed a significant decrease in P4HA1 expression in GC cells with TMEM45A knockdown, whereas P4HA1 expression was notably increased in GC cells with TMEM45A overexpression (Fig. 5H). Collectively, these results suggest that TMEM45A positively regulates P4HA1 expression in GC. To explore whether TMEM45A affects the proliferation, migration, and invasion capabilities of GC cells through P4HA1, functional rescue experiments were conducted. CCK-8 and EDU assays showed that TMEM45A knockdown significantly inhibited the proliferation of AGS and HGC-27 cells, while P4HA1 overexpression markedly promoted GC cell proliferation. Co-transfection of the TMEM45A knockdown

vector and P4HA1 overexpression vector partially reversed the inhibitory effect of TMEM45A knockdown on GC cell proliferation (Fig. 5I-J). Transwell and scratch wound healing assays revealed that TMEM45A knockdown significantly suppressed the migration and invasion of AGS and HGC-27 cells, whereas P4HA1 overexpression significantly enhanced GC cell migration and invasion. Similarly, co-transfection of the TMEM45A knockdown vector and P4HA1 overexpression vector partially rescued the inhibitory effect of TMEM45A knockdown on GC cell migration and invasion (Fig. 5K-L).

TMEM45A acts through the P4HA1/succinic acid/TGF-β pathway in GC

Based on the expression levels of TMEM45A and P4HA1 in TCGA database, we performed GSEA. The results revealed that TMEM45A and P4HA1 share a common signaling pathway, namely the TGF-β pathway (TMEM45A, *NES* = 1.937, *P* < 0.001; P4HA1, *NES* = 1.601, *P* < 0.05) (Fig. 6A). Previous studies have demonstrated that P4HA1, as an α-ketoglutarate (α-KG)-dependent dioxygenase, converts α-KG to succinate during its catalytic process of proline 4-hydroxylation [15]. Upregulated expression of P4HA1 leads to massive accumulation of succinate, which in turn contributes to GC progression [16]. Meanwhile, accumulating evidence has indicated that succinate can promote the activation of the TGF-β pathway [17]. Combined with the above experimental findings, we proposed the hypothesis that TMEM45A regulates the succinate/TGF-β pathway via P4HA1 in GC. Using a succinate detection kit, we observed that knockdown of TMEM45A significantly decreased the succinate concentration in GC cells, whereas overexpression of TMEM45A remarkably increased succinate levels in GC cells (Fig. 6B-C). To further validate our hypothesis, rescue experiments were conducted. The results showed that succinate concentration was significantly reduced after TMEM45A knockdown, and this reduction could be reversed by overexpressing P4HA1 (Fig. 6D). Additionally, Western blot analysis demonstrated that the level of phosphorylated Smad2/3 (p-Smad2/3) was significantly downregulated in TMEM45A-knockdown GC cells. Notably, overexpression of P4HA1 could abrogate the inhibitory effect of TMEM45A knockdown on p-Smad2/3 protein expression in GC cells (Fig. 6E). In conclusion, TMEM45A regulates the succinate/TGF-β/Smad signaling pathway through P4HA1 in GC.

Discussion

GC is a common malignant tumor worldwide, characterized by complex etiologies and high mortality. Currently, there remains a lack of efficient diagnostic and therapeutic strategies for this disease. Due to the insidious nature of early symptoms in GC patients, most are diagnosed at an advanced stage of the disease [18]. Furthermore, despite continuous advancements in systemic treatment modalities such as surgery, chemoradiotherapy, and pharmacotherapy, only a small subset of GC patients can derive clinical benefits from these interventions [19]. Therefore, there is an urgent need to identify effective biomarkers for GC diagnosis and prognosis. In recent years, with the progress of gene analysis technologies, a large number of key tumor-associated genes have been identified, and most of them can serve as potential

biomarkers or therapeutic targets for tumors. In this study, we first screened multiple GC-related datasets and predicted TMEM45A as a potential target gene in GC tissues.

Existing studies have demonstrated that TMEM45A is involved in the progression of various tumors and can serve as a marker for pathological lesions. For instance, in ovarian cancer, inhibition of TMEM45A has been shown to suppress tumor cell proliferation, induce cell cycle arrest, and reduce cell invasiveness [20]. Zhang et al. and Anna et al. proposed that the transcriptional level of TMEM45A could act as a predictive marker for high-grade cervical lesions [21]. Neuperger et al. were the first to identify TMEM45A as a marker for single-cell heterogeneity in adenocarcinomas; notably, TMEM45A is highly expressed in lung adenocarcinoma, and this finding has been validated using immunohistochemical methods [22]. In addition to its roles in tumors, TMEM45A has also been implicated in other diseases. For example, through a combination of bioinformatics analysis and experimental validation, Xu et al. found that TMEM45A in systemic lupus erythematosus can influence atrial fibrillation by regulating atrial fibrosis in SLE patients, thereby potentially exerting a therapeutic effect [23]. Another study by Cui et al. showed that in hormone receptor-positive (HR+) breast cancer, TMEM45A may serve as a potential therapeutic target to overcome palbociclib resistance and is associated with the process of cellular glycolysis [24]. However, the specific molecular mechanism underlying TMEM45A in the initiation and progression of GC remains unclear. To address this gap, the present study conducted a series of experimental investigations. First, the expression level of TMEM45A in GC tissues was predicted using multiple databases and subsequently validated via immunohistochemistry. The results revealed that the protein level of TMEM45A in GC tissues was significantly higher than that in adjacent non-tumor tissues, and its expression was significantly correlated with residual tumor status and the outcome of initial GC treatment. Subsequently, univariate and multivariate Cox regression analyses, along with nomogram construction, confirmed that TMEM45A is an independent prognostic factor for GC and can effectively predict the prognosis of GC patients. Furthermore, biological function studies indicated that TMEM45A is crucial for the proliferation and metastasis of GC cells.

To further explore the potential functional factors associated with TMEM45A, this study first performed an analysis using the SPRING database. Based on protein binding scores, P4HA1 was identified as the factor that binds most tightly to TMEM45A. P4HA1 is a well-known key enzyme in collagen synthesis and has been demonstrated to exert a significant pro-tumorigenic role in various cancers. In hypopharyngeal squamous cell carcinoma, P4HA1 can promote tumor cell migration and colonization [25]. In glioblastoma, P4HA1 serves as a poor prognostic marker; under hypoxic conditions, it can induce the epithelial-mesenchymal transition process, thereby enhancing tumor cell migration and invasion [26]. Additionally, a study by Ma et al. showed that targeting P4HA1 can promote the expansion of CD8 + T cell progenitors, which in turn enables immune memory and systemic anti-tumor immunity [16]. Xu et al. further found that hypoxia-induced overexpression of P4HA1 in endothelial cells can drive glycolytic metabolic reprogramming via the P4HA1/α-ketoglutarate (α-KG)/TET2/FBP1 pathway, ultimately facilitating angiogenesis. This study further verified the association and functional interaction between P4HA1 and TMEM45A in GC. Analysis of the Timer database and Western blot experiments confirmed

that TMEM45A positively regulates the expression of P4HA1. Functional experiments showed that overexpression of P4HA1 could abrogate the inhibitory effect of TMEM45A knockdown on the proliferation and metastatic capacity of GC cells in vitro. These results indicate that TMEM45A can promote the proliferation, migration, and invasion of GC cells by mediating P4HA1.

Numerous studies have confirmed that transforming growth factor-β (TGF-β), as a pleiotropic secreted cytokine, can regulate multiple biological processes such as cell proliferation, differentiation, invasion, migration, and apoptosis [27]. Existing studies have suggested a close association between TMEM45A and TGF-β signaling. Lan et al. found that in a renal fibrosis model, knockdown of TMEM45A significantly attenuated the TGF-β1-induced upregulation of extracellular matrix components and inflammatory cytokines [28]; Zhu et al. reported that knockdown of TMEM45A could reverse multidrug resistance in human colorectal cancer cells and inhibit their epithelial-mesenchymal transition by suppressing the TGF-β signaling pathway [29]. In this study, further analysis via GSEA revealed that TMEM45A and P4HA1 share a common downstream regulatory pathway, namely the TGF-β pathway. Meanwhile, existing studies have verified that P4HA1 can participate in tumor progression by regulating succinate: in glioblastoma, high expression of P4HA1 significantly increases intracellular succinate concentration, promoting succinate biosynthesis and protein succinylation [30]; in turn, succinate can further promote the activation of the TGF-β pathway by activating the GPR91 receptor [17].

Building on the conclusion previously confirmed in this study—where TMEM45A promotes the proliferation, migration, and invasion of GC cells by mediating P4HA1—and considering that no literature has yet reported the interaction between TMEM45A, succinate, and TGF-β in GC, this study proposes a core hypothesis. In GC, TMEM45A regulates the succinate/TGF-β/Smad signaling pathway through the mediation of P4HA1. To validate this hypothesis, relevant experiments results demonstrated that knockdown of TMEM45A in GC cells significantly reduced intracellular succinate content and decreased the phosphorylation level of Smad protein. In contrast, exogenous overexpression of P4HA1 alleviated the reduction in succinate content and the decrease in Smad phosphorylation level induced by TMEM45A knockdown, respectively.

Conclusions

This study demonstrates that TMEM45A functions as a positive regulator and a prognostic marker in GC. P4HA1, an interacting partner of TMEM45A, is highly expressed in GC tissues. Additionally, the study clarifies the molecular mechanism by which TMEM45A mediates the succinate/TGF-β/Smad pathway through P4HA1 in GC. Subsequent studies will involve animal experiments to provide further verification. These findings provide both a valid prognostic biomarker for GC and potential therapeutic targets for GC intervention.

Declarations

Author Contribution: All authors contributed to the conception and design of this study. Fei Ge and Rongrong Jing: Conception and design. Yan Wang, Ming Cui and Jingchun Wang: Administrative support. Ming Cui: Provision of study materials or patients. Fei Ge and Rui Ji: Collection and assembly of data. Fei Ge and Rui Ji: Data analysis and interpretation. Fei Ge: Manuscript writing. All authors commented on the previous versions of the manuscript, and all have read and approved the final version of the manuscript.

Competing interests: The authors declare no competing interests.

Funding: This study was supported by the Natural Science Foundation of Nantong Municipality of China (JC2023107) and Ili Kazakh Autonomous Prefecture Science and Technology Program (YJC2025A21).

Ethical Statement: The authors are accountable for all aspects of the work in ensuring that questions related to the accuracy or integrity of any part of the work are appropriately investigated and resolved. The study was conducted in accordance with the Declaration of Helsinki and its subsequent amendments. The study was approved by the Ethical Committee of the Affiliated Hospital of Nantong University (2024-K078-01). Informed consent was obtained from all individual participants or their legal guardians, including for the use of any tissue samples.

Data availability: The data that support the findings of this study are available from the corresponding author upon reasonable request.

References

1. Yang, W. J. et al. Updates on global epidemiology, risk and prognostic factors of gastric cancer. *World J. Gastroenterol.* **29**, 2452 (2023).
2. Smyth, E. C., Nilsson, M., Grabsch, H. I., van Grieken, N. C. & Lordick, F. Gastric cancer. *Lancet* **396**, 635–648 (2020).
3. Correa, P. Gastric cancer: overview. *Gastroenterol. Clin. N. Am.* **42**, 211 (2013).
4. Varadhachary, G. & Ajani, J. A. Gastric cancer. *Clinical advances in hematology & oncology: H&O* 3, 118–124 (2005).
5. Zhang, L. H. et al. Vestigial like family member 3 is a novel prognostic biomarker for gastric cancer. *World journal of clinical cases* 7, (2019). (1954).
6. Crew, K. D. & Neugut, A. I. Epidemiology of gastric cancer. *World J. gastroenterology: WJG*. **12**, 354 (2006).
7. Berretta, M. et al. The role of diet in gastric cancer: still an open question. *Front. Biosci.* **17**, 7 (2012).
8. Shang, J. & Pena, A. Multidisciplinary approach to understand the pathogenesis of gastric cancer. *World J. Gastroenterology: WJG*. **11**, 4131 (2005).
9. Schmit, K. & Michiels, C. TMEM proteins in cancer: a review. *Front. Pharmacol.* **9**, 1345 (2018).

10. Hayez, A. et al. High TMEM 45A expression is correlated to epidermal keratinization. *Exp. Dermatol.* **23**, 339–344 (2014).
11. Sun, W. et al. Knockdown of TMEM45A inhibits the proliferation, migration and invasion of glioma cells. *Int. J. Clin. Exp. Pathol.* **8**, 12657 (2015).
12. Flamant, L. et al. TMEM45A is essential for hypoxia-induced chemoresistance in breast and liver cancer cells. *BMC cancer*. **12**, 391 (2012).
13. Liu, Y., Liu, L. & Mou, Z. X. TMEM45A affects proliferation, apoptosis, epithelial-mesenchymal transition, migration, invasion and cisplatin resistance of HPV-positive cervical cancer cell lines. *Biochem. Genet.* **60**, 173–190 (2022).
14. Jiang, H., Chen, H., Wan, P., Liang, M. & Chen, N. Upregulation of TMEM45A promoted the progression of clear cell renal cell carcinoma in vitro. *Journal Inflamm. research*, 6421–6430 (2021).
15. Xiong, G. et al. Collagen prolyl 4-hydroxylase 1 is essential for HIF-1α stabilization and TNBC chemoresistance. *Nat. Commun.* **9**, 4456 (2018).
16. Ma, S. et al. Targeting P4HA1 promotes CD8 + T cell progenitor expansion toward immune memory and systemic anti-tumor immunity. *Cancer Cell.* **43**, 213–231 (2025).
17. Xie, L. et al. Suppressing MASH fibrotic progression by blocking succinate-GPR91 signaling in hepatic stellate cells. *Hepatology* **10**, 1097 (2025).
18. Lordick, F. et al. Gastric cancer: ESMO Clinical Practice Guideline for diagnosis, treatment and follow-up. *Ann. Oncol.* **33**, 1005–1020 (2022).
19. Guan, W. L., He, Y. & Xu, R. H. Gastric cancer treatment: recent progress and future perspectives. *J. Hematol. Oncol.* **16**, 57 (2023).
20. Guo, J. et al. Inhibition of TMEM45A suppresses proliferation, induces cell cycle arrest and reduces cell invasion in human ovarian cancer cells. *Oncol. Rep.* **33**, 3124–3130 (2015).
21. Manawapat-Klopfer, A. et al. TMEM45A, SERPINB5 and p16INK4A transcript levels are predictive for development of high-grade cervical lesions. *Am. J. cancer Res.* **6**, 1524 (2016).
22. Neuperger, P. et al. Analysis of the single-cell heterogeneity of adenocarcinoma cell lines and the investigation of intratumor heterogeneity reveals the expression of transmembrane protein 45A (TMEM45A) in lung adenocarcinoma cancer patients. *Cancers* **14**, 144 (2021).
23. Xu, H. et al. Integrated bioinformatics and validation reveal TMEM45A in systemic lupus erythematosus regulating atrial fibrosis in atrial fibrillation. *Mol. Med.* **31**, 104 (2025).
24. Chen, C. et al. TMEM45A enhances palbociclib resistance and cellular glycolysis by activating AKT/mTOR signaling pathway in HR+ breast cancer. *Cell. death discovery*. **11**, 47 (2025).
25. Sato, K. et al. P4HA1 Promotes Cell Migration and Colonization in Hypopharyngeal Squamous Cell Carcinoma. *Anticancer Res.* **43**, 2571–2582 (2023).
26. Zhu, X. et al. P4HA1 as an unfavorable prognostic marker promotes cell migration and invasion of glioblastoma via inducing EMT process under hypoxia microenvironment. *Am. J. Cancer Res.* **11**, 590 (2021).

27. Ali, S. et al. TGF-β signaling pathway: Therapeutic targeting and potential for anti-cancer immunity. *Eur. J. Pharmacol.* **947**, 175678 (2023).
28. Lan, J. et al. TMEM45A is involved in renal fibrosis in rats by regulating Jagged1/Notch pathway. *Front. Bioscience-Landmark*. **25**, 593–605 (2020).
29. Zhu, M. et al. Knockdown of TMEM45A overcomes multidrug resistance and epithelial–mesenchymal transition in human colorectal cancer cells through inhibition of TGF-β signalling pathway. *Clin. Exp. Pharmacol. Physiol.* **47**, 503–516 (2020).
30. Yang, S. et al. HIF1α/ATF3 partake in PGK1 K191/K192 succinylation by modulating P4HA1/succinate signaling in glioblastoma. *Neuro-oncology* 26, 1405–1420 (2024).

Scheme 1

Scheme 1 is available in the Supplementary Files section.

Figures

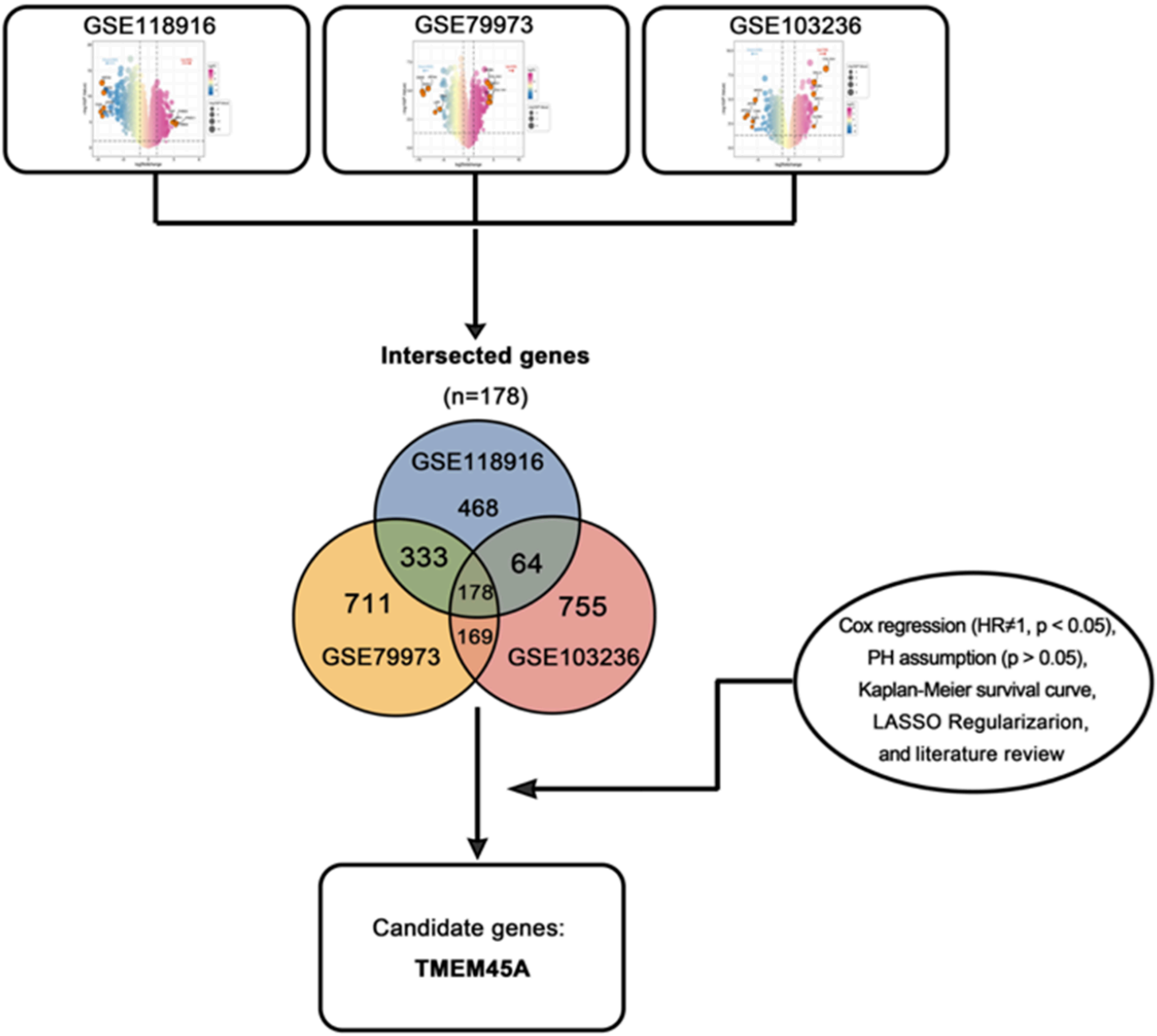


Figure 1

Screening for differentially expressed gene TMEM45A in GC.

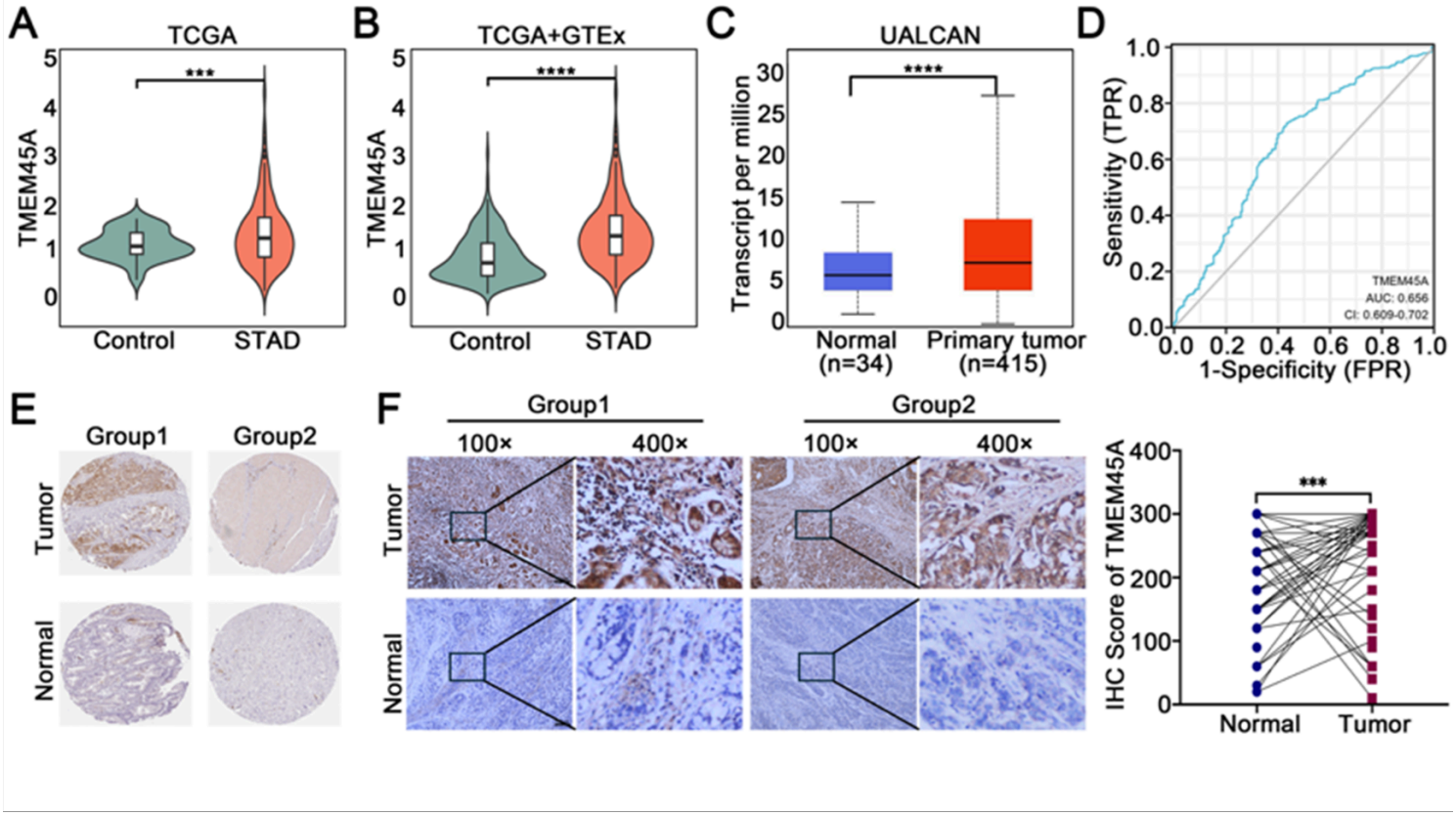


Figure 2

TMEM45A is highly upregulated in GC and correlates with clinical features. (A) Expression of TMEM45A in normal gastric tissue samples versus GC tissue samples from the TCGA database. (B) Expression of TMEM45A in normal gastric tissue samples versus GC tissue samples from the combined TCGA + GTEx databases. (C) Expression of TMEM45A in normal gastric tissue samples versus GC tissue samples from the UALCAN database. (D) ROC curve of TMEM45A in GC. (E) Protein expression of TMEM45A in normal gastric tissues and GC tissues from the HPA database. (F) Verification of TMEM45A protein expression in 75 pairs of clinical GC tissue samples by immunohistochemistry. Data are expressed as mean ± SD. **** $P < 0.0001$, *** $P < 0.001$, ** $P < 0.01$, * $P < 0.05$.

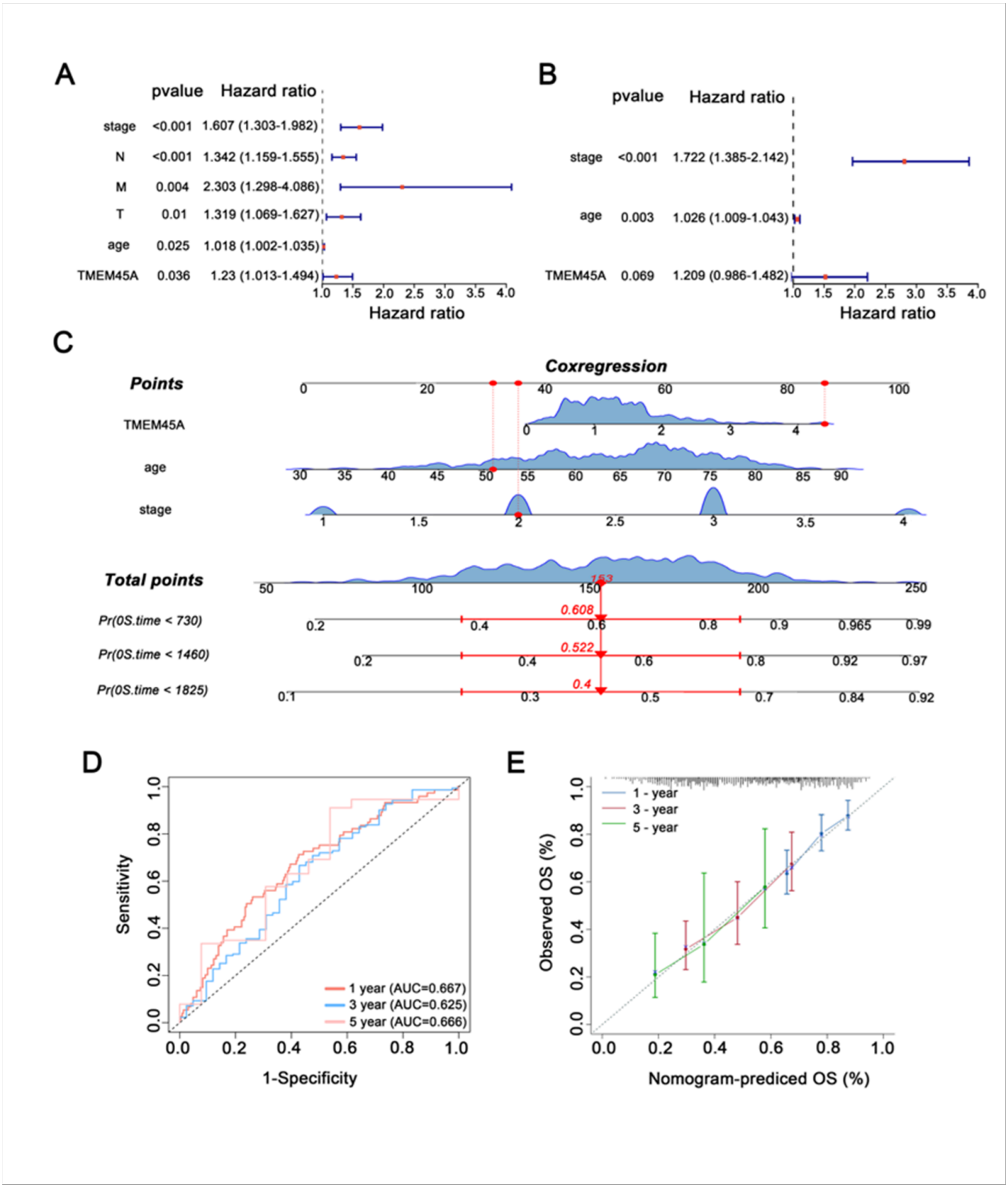


Figure 3

TMEM45A serves as a prognostic marker in GC. (A) Univariate Cox regression analysis of TMEM45A showed that the factors influencing the survival of GC patients included stage, N stage, M stage, T stage, age, and TMEM45A expression level. (B) Multivariate Cox regression analysis of TMEM45A showed that the factors influencing the survival of GC patients included stage, age, and TMEM45A expression level. (C) Nomogram based on TMEM45A expression for predicting the overall survival of GC patients. (D) ROC

curves and calculated area under the curve (AUC) values for predicting the 1-, 3-, and 5-year prognosis of GC patients using the nomogram. (E) Calibration curves of the nomogram for predicting the 1-, 3-, and 5-year survival rates. All error bars represent the confidence interval (CI, 95%). **** $P < 0.0001$, *** $P < 0.001$, ** $P < 0.01$, * $P < 0.05$.

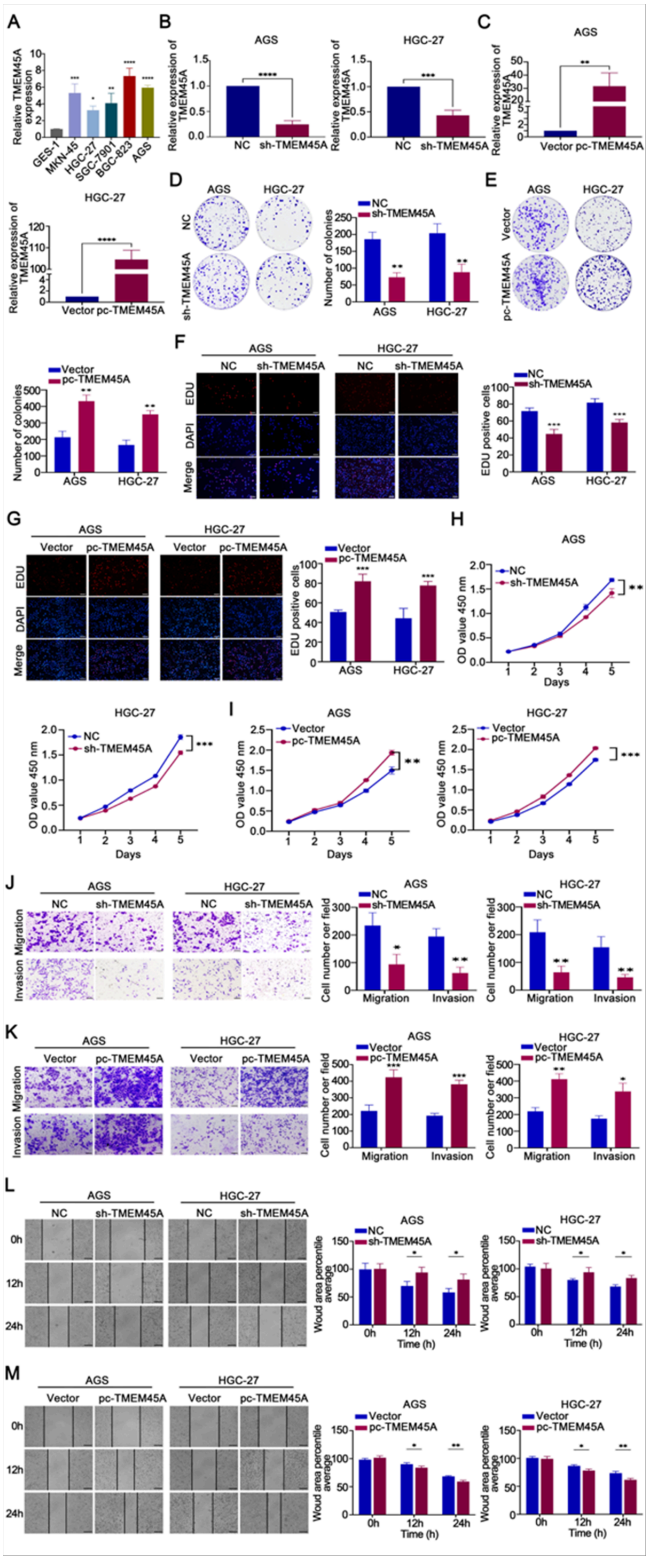


Figure 4

TMEM45A promotes proliferation, migration, and invasion in GC. (A) Expression of TMEM45A in GC cells. (B-C) Knockdown and overexpression efficiency of TMEM45A in AGS and HGC-27 GC cells. Colony formation assay (D-E), EdU assay (F-G), and CCK-8 assay (H-I) verifying the effect of TMEM45A knockdown and overexpression on the proliferative capacity of GC cells (scale bar, 50 μm). Transwell assay (J-K) and wound healing assay (L-M) verifying the effect of TMEM45A knockdown and overexpression on the migration and invasion of GC cells (scale bar, 100 μm). All quantitative data are presented as the mean ± SD from three replicates of three independent experiments. **** $P < 0.0001$, *** $P < 0.001$, ** $P < 0.01$, * $P < 0.05$.

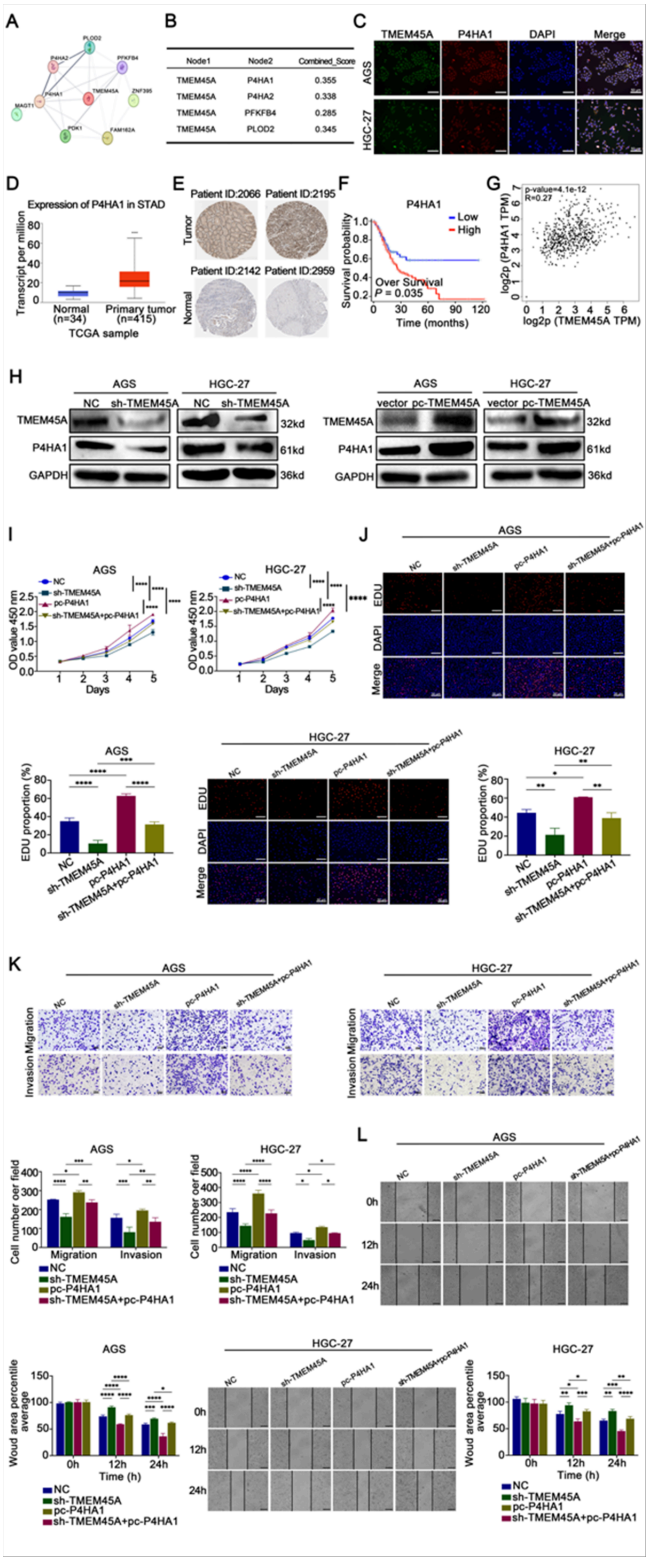


Figure 5

TMEM45A binds to P4HA1 to promote the proliferation, migration, and invasion of GC. (A) PPI network of TMEM45A and its interacting proteins, analyzed using the STRING database. (B) Among the interacting proteins, P4HA1 showed the highest binding score based on binding score analysis. (C) Immunofluorescence assay was used to detect the co-localization of TMEM45A and P4HA1 expression in AGS and HGC-27 GC cells (scale bar, 50 μm). (D) Expression of P4HA1 in 34 normal gastric tissue

samples and 415 GC tissue samples from the TCGA database. (E) Protein expression of TMEM45A in normal gastric tissues and GC tissues from the HPA database. (F) Kaplan-Meier survival curves of GC patients with high or low P4HA1 expression. (G) Scatter plot showing the correlation between TMEM45A and P4HA1 expression levels in GC tissues, based on the TIMER database. A direct correlation was observed between TMEM45A and P4HA1 expression in GC tissues, with a correlation coefficient of R = 0.27 ($P < 0.05$). (H) Western blot assay verified a positive correlation between TMEM45A and P4HA1 in GC. CCK-8 assay (I) and EdU assay (J) verified that TMEM45A binding to P4HA1 promoted the proliferative capacity of GC cells (scale bar, 50 μm). Transwell assay (K) and wound healing assay (L) verified that TMEM45A binding to P4HA1 promoted the migration and invasion capabilities of GC cells (scale bar, 100 μm). All quantitative data are presented as the mean ± SD from three replicates of three independent experiments. **** $P < 0.0001$, *** $P < 0.001$, ** $P< 0.01$, * $P < 0.05$.

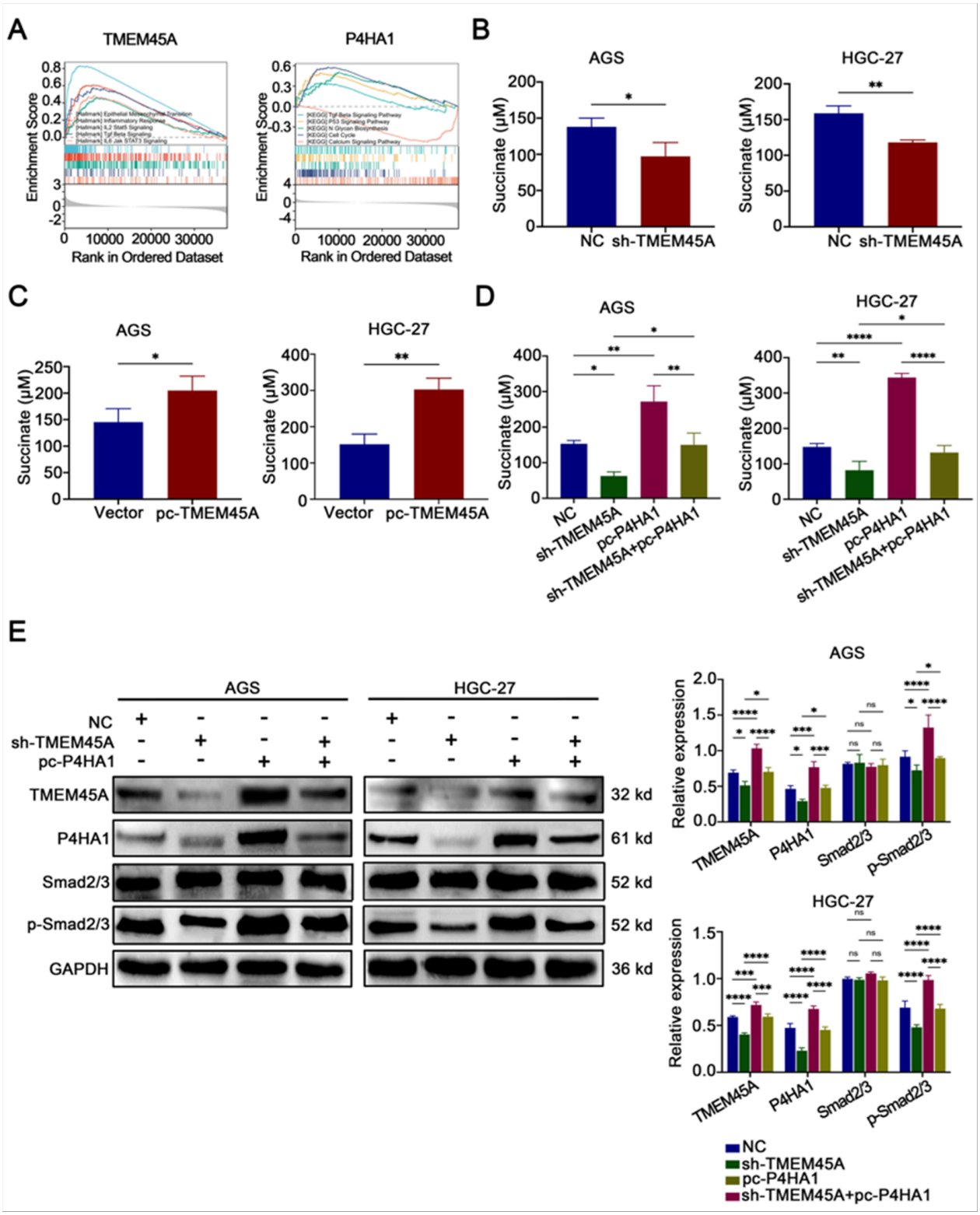


Figure 6

TMEM45A Mediates the Succinate/TGF-β/Smad Signaling Pathway via P4HA1 in GC. (A) GSEA of TMEM45A and P4HA1 in GC tissue samples from the TCGA database. (B) Effect of TMEM45A knockdown and overexpression on succinate levels in GC cells. (D) Effect of TMEM45A on succinate levels in GC cells via P4HA1. (E) Western blot assay analyzed the protein levels of TMEM45A, P4HA1, Smad2/3, and p-Smad2/3 in GC cells with TMEM45A knockdown and subsequent P4HA1

overexpression. All quantitative data are presented as the mean ± SD from three replicates of three independent experiments. **** $P < 0.0001$, *** $P < 0.001$, ** $P < 0.01$, * $P < 0.05$.

Supplementary Files

This is a list of supplementary files associated with this preprint. Click to download.

- ID37be72424e644334a3c53c47848af296Fig5HFig6EWBRawDataAnnotations.pdf
- floatimage1.png